Development of computationally efficient biorthogonal wavelets

Mehmet Cemil KALE[*]

Eskişehir Vocational School, Eskişehir Osmangazi University, Eskişehir, Turkey

Abstract: Daubechies 5-tap/3-tap (Daub 5/3) wavelet and Kale 5-tap/3-tap (Kale 5/3) wavelet are computationally efficient wavelets which can be implemented by bitwise shifts and additions in the lifting scheme. In this work, presented is a formulation for computationally efficient wavelet prediction (P) and update (U) filters of two-channel lifting structures. Their subband decomposition scheme counterparts are also given. This research bases itself on the Daub 5/3 and Kale 5/3 wavelets and develops a formula for wavelets (which can be implemented with bitwise shifts and additions) that are derived from these two wavelets. The proposed wavelets are tried on 16 test images for three-level wavelet decompositions and better decorrelation results are achieved for the proposed wavelets for higher-level decompositions.

Key words: Biorthogonal wavelets, lifting scheme, filter banks, filter design, integer-to-integer wavelet transform

1. Introduction

In addition to the classical subband filtering structure, lifting scheme is widely popular for discrete wavelet transform because of its design flexibility [1–5]. The discrete wavelet transform applies two different filters to the same signal. On the other hand, for the lifting scheme, the signal is divided into two (namely into odd and even indices). Then a chain of convolution and accumulation operations across these two signals are applied.

Extensive investigation has also been done for the development of a technique to define the wavelet transform as a transform matrix: block wavelet transform (BWT) [6–8]. Instead of a conventional discrete wavelet transform, the discrete wavelet transform is achieved using matrix multiplications.

The first research of the author consisted of the iterative development of a $2^N \times 2^N$ BWT matrix development algorithm (from smaller BWT counterparts) and the design of a filter by considering the orthogonality limitations of BWT matrices of the lifting scheme. In the same research, the author proposed another filter whose output BWT matrices converged to the Karhunen-Loéve transform matrices of test images [7, 8]. Here, there was a problem: The wavelets were signal-dependent. The second research of the author fixed this problem by declaring a general and computationally efficient Kale 5-tap/3-tap (Kale 5/3) wavelet [9].

In the area of integer-to-integer wavelet transforms, Adams and Kossentni made a performance evaluation and analysis for image compression [10]. In addition, Calderbank et al. designed their famous wavelet transforms that map integers to integers [11, 12]. Other integer-to-integer wavelet transform studies can be listed as follows: [13–19]. This research investigates an integer-to-integer wavelet transform methodology which bases itself on the Daubechies 5-tap/3-tap (Daub 5/3) wavelet and Kale 5/3 wavelet as the first- and second-degree wavelets respectively and constructs the following degree wavelets using the relationship between Daub 5/3 and Kale

---

[*]Correspondence: kale.14@osu.edu

5/3 wavelets.

The Daub 5/3 wavelet can be realized in the lifting scheme with bitwise additions and shifts and so can the Kale 5/3 wavelet [9, 11, 20]. This property makes these wavelets computationally efficient. The motivation behind this research is to answer this question: "Can there be a formulation for the computationally effective wavelet design?" The author has found that there is indeed a formulation for the purpose and more wavelets can be designed. Using that formulation, the user can pick an arbitrary degree of a wavelet and the wavelet will still be computationally efficient and wavelet transforms can be achieved using bitwise additions and shifts.

The paper starts with the lifting scheme in Section 2. The lifting scheme is followed by the description of the Daubechies 5-tap/3-tap (Daub 5/3) wavelet. Section 4 presents the description of the Kale 5-tap/3-tap (Kale 5/3) wavelet. Section 5 formulizes the computationally efficient wavelet design and then presents the results.

2. Lifting scheme

Lifting is both a wavelet design and a discrete wavelet transform technique [1–3]. The lifting scheme separates discrete wavelet transform (DWT) using finite filters into a group of elementary convolution operators. These convolution operators are called the lifting steps.

Because the downsampling operation precedes the filtering, lifting scheme reduces the number of arithmetic operations approximately by two. The analysis operation of the lifting scheme is shown in Figure 1. A very convenient way of the lifting scheme is that the synthesis operation is completely symmetric to the analysis operation.
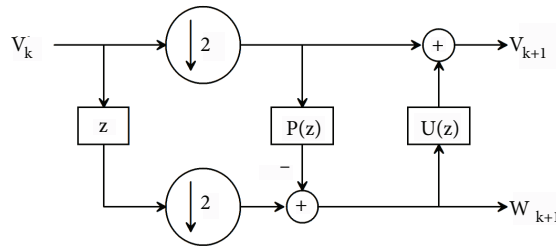
Figure 1. 1-level lifting analysis operation.

The lifting scheme uses biorthogonal wavelets as an alternative method for accomplishing the DWT. The lifting and scaling steps are generated from the biorthogonal wavelets in order to perform the DWT using the lifting scheme. In the lifting scheme, the polyphase matrix is described as

$$\mathbf{H}_p = \left[\begin{array}{cc} H_{0,ev}(z) & H_{0,od}(z) \\ H_{1,ev}(z) & H_{1,od}(z) \end{array} \right]$$

The polyphase matrix is a 2×2 matrix which contains the low-pass and high-pass analysis filters. Each of these filters are divided into their even and odd polynomial coefficients. Of the polyphase matrix, these

coefficients are

$$
\begin{aligned}
H_{0,ev}(z) &= 1 - P(z)U(z) \\
H_{0,od}(z) &= U(z) \\
H_{1,ev}(z) &= -P(z) \\
H_{1,od}(z) &= 1
\end{aligned}
\tag{1}
$$

where the subband analysis filters are

$$
\begin{aligned}
H_0(z) &= H_{0,ev}(z^2) + zH_{0,od}(z^2) \\
&= 1 - P(z^2)U(z^2) + zU(z^2) \\
H_1(z) &= H_{1,ev}(z^2) + zH_{1,od}(z^2) \\
&= -P(z^2) + z
\end{aligned}
\tag{2}
$$

and the subband synthesis filters are

$$
\begin{aligned}
G_0(z) &= -z^{-1}H_1(-z) \\
G_1(z) &= z^{-1}H_0(-z)
\end{aligned}
\tag{3}
$$

Wavelets must have at least one vanishing moment in order to have their scaling and dilation equations to converge. This can only be achieved when

$$
\begin{aligned}
H_0(-1) &= 0 \\
H_1(1) &= 0
\end{aligned}
\tag{4}
$$

If the prediction $P(z)$ and update $U(z)$ filters are in the form

$$
\begin{aligned}
P(z) &= \sum_i \alpha_i z^{-i} \\
U(z) &= \sum_i \beta_i z^{-i}
\end{aligned}
\tag{5}
$$

it must be made sure that

$$
\begin{aligned}
\alpha &= \sum_i \alpha_i = 1 \\
\beta &= \sum_i \beta_i = 0.5
\end{aligned}
\tag{6}
$$

The lifting scheme operates in a perfect reconstruction environment. The synthesis is done with the inverse of the polyphase matrix described in the above paragraphs [1–3]. None of the proposed wavelets described in the below sections violates the perfect reconstruction character of the lifting scheme. This research focuses on the design of the prediction $P(z)$ and update $U(z)$ contents which will not make structural changes to the analysis and synthesis stages of the lifting scheme; thus, the perfect reconstruction is preserved.

3. First degree: Daubechies 5-tap/3-tap (Daub 5/3) wavelet

The Daubechies wavelets, which are based on the extensive studies of Ingrid Daubechies, are a group of orthogonal and biorthogonal wavelets. As a discrete wavelet transform technique, the Daubechies wavelets possess the maximal number of vanishing moments for some given support. In each wavelet of this group, there is a scaling function which is also called the father wavelet [21, 22]. The father wavelet generates an orthogonal or a biorthogonal multiresolution analysis [11, 20]. Our case is biorthogonal wavelet design; thus, we may focus on one of the most famous biorthogonal wavelets of Ingrid Daubechies: The Daubechies 5-tap/3-tap wavelet.

Daubechies 5-tap/3-tap (Daub 5/3) wavelet has the following subband analysis/synthesis filters:

$$
\begin{aligned}
H_0^{(1)}(z) &= \frac{1}{8}(-z^2 + 2z + 6 + 2z^{-1} - z^{-2}) \\
H_1^{(1)}(z) &= \frac{1}{2}(-z^2 + 2z - 1)
\end{aligned}
\tag{7}
$$

$$
\begin{aligned}
G_0^{(1)}(z) &= \frac{1}{2}(2z + 1 + 2z^{-1}) \\
G_1^{(1)}(z) &= \frac{1}{8}(-z - 2 + 6z^{-1} - 2z^{-2} - z^{-3})
\end{aligned}
\tag{8}
$$

and the following prediction $P(z)$ and update $U(z)$ filters:

$$
\begin{aligned}
P^{(1)}(z) &= \frac{1}{2} + \frac{1}{2}z \\
U^{(1)}(z) &= \frac{1}{4} + \frac{1}{4}z^{-1}
\end{aligned}
\tag{9}
$$

The prediction and update implementation of the Daub 5/3 wavelet can be implemented using bitwise shifts and additions. This makes the Daub 5/3 wavelet computationally efficient. The general wavelet proposed by Kale possesses such properties [9].

4. Second degree: Kale 5-tap/3-tap (Kale 5/3) wavelet

Although not having vanishing moments as much as Daub 5/3 wavelet, Kale have proposed a general wavelet as shown in Equation 10 which has plausible regularity properties and also provides better decorrelation performances than the Daub 5/3 wavelet on 16 test images [9].

$$
\begin{aligned}
P^{(2)}(z) &= \frac{3}{4} + \frac{1}{4}z \\
U^{(2)}(z) &= \frac{7}{16} + \frac{1}{16}z^{-1}
\end{aligned}
\tag{10}
$$

As shown in Equation 11, these prediction and update filters can be explained using bitwise additions and shifts as in Daub 5/3.

$$
\begin{aligned}
P^{(2)}(z) &= 1 - \frac{1}{4} + \frac{1}{4}z \\
U^{(2)}(z) &= \frac{1}{2} - \frac{1}{16} + \frac{1}{16}z^{-1}
\end{aligned}
\tag{11}
$$

The scalar components (i.e. 1, -1/4, 1/2, and -1/16) and delayer components (i.e. $z/4$ and $z^{-1}/16$) are simple bitwise shift operations. The wavelet introduced by Kale has shiftings of 4 for prediction (1/4 and $z/4$) and 9 for update (1/2, 1/16 and $z^{-1}/16$) [9] compared to the Daubechies' bitwise shifts of 2 for prediction (i.e. 2 for 1/2 and $z/2$) and 4 for update (i.e. 4 for 1/4 and $z^{-1}/4$). Moreover, there are 2 addition operations for prediction and another 2 addition operations for update realizations compared to the Daubechies' 1 addition for prediction and 1 addition for update.

The lifting scheme filters of Equation 10 issue analysis subband wavelets such as

$$
\begin{aligned}
H_0^{(2)}(z) &= \frac{1}{64}\left(-7z^2 + 28z + 42 + 4z^{-1} - 3z^{-2}\right) \\
H_1^{(2)}(z) &= \frac{1}{4}\left(-z^2 + 4z - 3\right)
\end{aligned}
\tag{12}
$$

and the subband scheme filters of the synthesis become

$$
\begin{aligned}
G_0^{(2)}(z) &= -z^{-1}H_1(-z) \\
&= \frac{1}{4}\left(z + 4 + 3z^{-1}\right) \\
G_1^{(2)}(z) &= z^{-1}H_0(-z) \\
&= \frac{1}{64}\left(-7z - 28 + 42z^{-1} - 4z^{-2} - 3z^{-3}\right)
\end{aligned}
\tag{13}
$$

5. Following degrees

The Daub 5/3 wavelet represents the first-degree computationally efficient biorthogonal wavelet and the Kale 5/3 wavelet represents the second-degree computationally efficient biorthogonal wavelet. The main purpose of this research is to achieve the following degrees. These computationally efficient biorthogonal wavelets are given in this section. In order to generate the algorithm, the scope of interest would be the third-degree computationally efficient wavelet.

The third-degree computationally efficient 5-tap/3-tap wavelet would be

$$
\begin{aligned}
P^{(3)}(z) &= \frac{7}{8} + \frac{1}{8}z \\
U^{(3)}(z) &= \frac{31}{64} + \frac{1}{64}z^{-1}
\end{aligned}
\tag{14}
$$

or to write it more suitably

$$
\begin{aligned}
P^{(3)}(z) &= 1 - \frac{1}{8} + \frac{1}{8}z \\
U^{(3)}(z) &= \frac{1}{2} - \frac{1}{64} + \frac{1}{64}z^{-1}
\end{aligned}
\tag{15}
$$

The subband analysis filters become

$$H_0^{(3)}(z) = \frac{1}{512}\left(-31z^2 + 248z + 294 + 8z^{-1} - 7z^{-2}\right)$$

$$H_1^{(3)}(z) = \frac{1}{8}\left(-z^2 + 8z - 7\right)$$

(16)

and the subband scheme filters of the synthesis become

$$G_0^{(3)}(z) = -z^{-1}H_1(-z)$$

$$= \frac{1}{8}\left(z + 8 + 7z^{-1}\right)$$

$$G_1^{(3)}(z) = z^{-1}H_0(-z)$$

$$= \frac{1}{512}\left(-31z - 248 + 294z^{-1} - 8z^{-2} - 7z^{-3}\right)$$

(17)

Here there are 6 bitwise shifts for P ($1/8$ and $z/8$) and 13 bitwise shifts for U ($1/2$, $1/64$ and $z^{-1}/64$). By describing the third-degree computationally efficient wavelet, the general formula can be generated. Considering the previous degree wavelets, the general formula for the filters can be written as

$$P^{(i)}(z) = 1 - \frac{1}{2^i} + \frac{1}{2^i}z$$

$$U^{(i)}(z) = \frac{1}{2} - \frac{1}{4^i} + \frac{1}{4^i}z^{-1}$$

(18)

$$H_0^{(i)}(z) = \frac{1}{(2^3)^i}(-(2.4^{i-1} - 1)z^2 + (4.8^{i-1} - 2^i)z$$

$$+ 6.7^{i-1} + 2^i z^{-1} - (2^i - 1)z^{-2})$$

$$H_1^{(i)}(z) = \frac{1}{2^i}\left(-z^2 + 2^i z + 1 - 2^i\right)$$

(19)

$$G_0^{(i)}(z) = -z^{-1}H_1(-z)$$

$$= \frac{1}{2i}(z + 2^i + (2^i - 1)z^{-1})$$

$$G_1^{(i)}(z) = z^{-1}H_0(-z)$$

$$= \frac{1}{(2^3)^i}(-(2 \times 4^{i-1} - 1)z - (4 \times 8^{i-1} - 2^i)$$

$$+ 6 \times 7^{i-1}z^{-1} - 2^i z^{-2} - (2^i - 1)z^{-3})$$

(20)

In general, we can state that an i degree wavelet has $2i$ bitwise shifts for P and $4i + 1$ bitwise shifts for U. The number of addition operations do not change. Table 1 shows the number of shift and addition operations in detail.

Table 1. Numbers of shifts and additions for each degrees of wavelets.

Degree	P	U
1	2 shifts & 1 addition	4 shifts & 1 addition
2	4 shifts & 2 additions	9 shifts & 2 additions
3	6 shifts & 2 additions	13 shifts & 2 additions
$\vdots$	$\vdots$	$\vdots$
i	2i shifts & 2 additions	4i+1 shifts & 2 additions
$\vdots$	$\vdots$	$\vdots$

In order to give an idea for the higher degrees

$$\lim_{i \to \infty} P^{(i)}(z) = 1$$

$$\lim_{i \to \infty} U^{(i)}(z) = \frac{1}{2} \tag{21}$$

Hence, if we want to investigate the wavelets' behavior for $i \to \infty$, we can state that

$$\lim_{i \to \infty} H_0^{(i)}(z) = \frac{1}{2} + \frac{1}{2}z$$

$$\lim_{i \to \infty} H_1^{(i)}(z) = z - 1$$

$$\lim_{i \to \infty} G_0^{(i)}(z) = 1 + z^{-1} \tag{22}$$

$$\lim_{i \to \infty} G_1^{(i)}(z) = \frac{1}{2}z^{-1} - \frac{1}{2}$$

For higher degrees, not only the lifting scheme but also the subband decomposition scheme (i.e. $1/2$, $z/2$, z, - 1, 1, z^{-1}, $z^{-1}/2$, and -1/2) can be implemented using simple bitwise shift and addition operations.

To help readers comprehend the scaling and wavelet functions, the frequency responses of all degree scaling and wavelet functions are displayed in Figures 2 and 3. Moreover, the frequency responses of Patil' s 2 bit and 4 bit 5/3 wavelets are shown as PSPG 2 and PSPG 4, respectively [21, 22]. Le Gall' s 5/3 wavelet is

not included because it has the same frequency response as the Degree 1 (Daub 5/3) wavelet; thus, Le Gall 5/3 wavelet is represented with Degree 1 (Daub 5/3) wavelet [23].
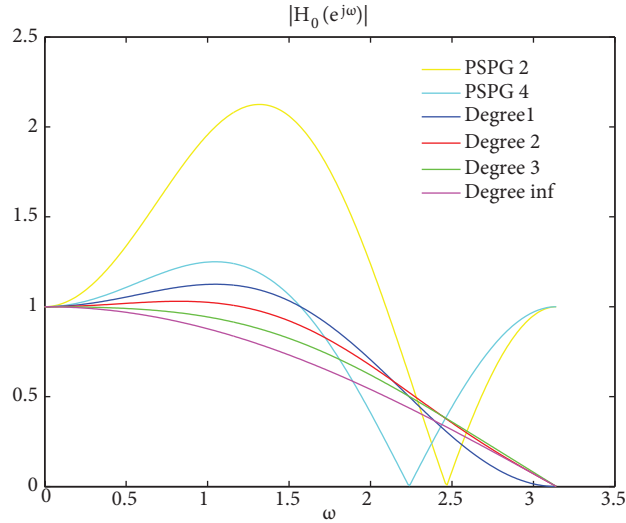
Figure 2. Frequency responses of $|H_0(e^{j\omega})|$ for all degree wavelets.
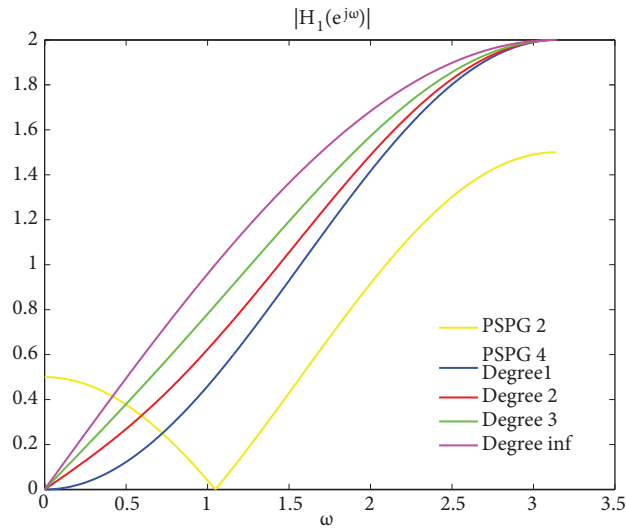
Figure 3. Frequency responses of $|H_1(e^{j\omega})|$ for all degree wavelets.

Degree 1 (Daub 5/3) wavelet seems to have the best curve because of its highest number of vanishing moments. However, other degree wavelets also prove to have better decorrelation results as can be seen in the next section. Note that $|H_1(e^{j\omega})|$ frequency response is the same for PSPG 4 (4 bit Patil 5/3) wavelet and Degree 1 (Daub 5/3) wavelet.

6. Results

As datasets, there are 16 test images. The images *Lena** and *Mandrill** are canny edge detection over original *Lena* and *Mandrill* images, respectively. On the other hand, *Bus** and *Foreman** are frame differences of the famous *Bus* and *Foreman* video sequences, respectively. In order to observe the decorrelation performances of the wavelets introduced in this paper, the variances of the outcomes (that are obtained in 3 level lifting decompositions) are calculated and listed in Tables 2 and 3. The L/H variance ratios are desired to be maximized.

Table 2. Variances of the wavelet tree images after three-level decomposition (Images 1-8).

Test image, Degree i	LLLL	LLLH	LLHL	LLHH	LLH	LHL	LHH	LH	HL	HH
Aerial, i=1	1474.75	927.91	1316.4	1730.7	489.75	812.23	575.57	110.45	192.70	60.402
Aerial, i=2	1147.75	595.03	803.03	1226.74	441.27	693.76	527.72	147.36	248.71	92.33
Aerial, i=3	950.01	459.77	622.091	937.265	418.518	631.614	527.242	189.883	310.016	145.604
Aerial, i→∞	845.493	444.334	600.116	841.448	432.953	627.863	602.742	247.986	395.137	243.692
1st Plane, i=1	2322.74	747.636	603.588	532.46	186.485	259.872	116.906	48.5499	85.0399	10.9563
1st Plane, i=2	2002.32	437.057	419.323	380.71	181.419	264.845	117.483	82.6466	106.396	17.6138
1st Plane, i=3	1810.46	338.545	426.645	342.322	194.729	274.025	129.892	114.887	131.601	29.0483
1st Plane, i→∞	1707.46	369.411	531.482	360.59	231.329	307.165	162.78	157.329	166.474	50.6679
2nd Plane, i=1	580.353	321.072	310.957	242.338	134.552	114.132	79.011	19.8558	23.0125	20.4354
2nd Plane, i=2	475.771	132.006	113.617	165.385	123.8	111.163	66.9966	23.629	29.3979	28.3982
2nd Plane, i=3	407.832	93.3917	74.0332	138.283	116.919	105.319	65.8411	29.3041	35.24	39.4793
2nd Plane, i→∞	383.712	127.443	108.398	145.056	121.375	107.354	74.5404	37.7735	43.113	58.3611
Barbara, i=1	2171.94	369.743	259.986	277.296	536.058	148.513	623.975	472.443	34.799	75.5528
Barbara, i=2	1986.21	260.59	178.464	231.889	423.452	140.82	518.516	472.849	51.3802	131.041
Barbara, i=3	1865.93	256.95	163.781	184.232	351.748	134.636	449.898	489.335	68.9417	215.574
Barbara, i→∞	1794.68	307.056	184.889	172.346	318.521	138.73	407.004	531.058	88.6745	359.426
Bus*, i=1	399.856	1216.95	332.905	1145.89	1880.08	563.4	1688.61	2412.79	221.111	453.78
Bus*, i=2	236.097	933.059	229.243	705.079	1514.98	434.68	1380.21	2461.03	258.386	649.34
Bus*, i=3	152.791	703.602	157.557	493.694	1281.11	338.548	1174.42	2561.64	301.135	935.023
Bus*, i→∞	103.789	556.131	112.461	397.022	1130.91	273.212	1067.83	2755.65	354.185	1401.54
Elaine, i=1	2329.48	286.069	268.352	210.787	109.29	121.275	84.1716	26.867	47.5747	110.481
Elaine, i=2	2115.84	209.891	155.34	170.111	112.564	122.161	73.3208	35.4041	53.7308	125.469
Elaine, i=3	1983.44	211.95	150.311	157.921	120.513	124.136	70.4157	45.0581	60.4423	146.426
Elaine, i→∞	1910.74	264.714	201.783	179.223	141.539	138.092	78.5744	58.0226	69.8929	179.732
Foreman*, i=1	3.9733	20.391	8.8136	45.206	41.385	16.918	50.441	58.892	9.7729	21.404
Foreman*, i=2	2.6965	12.511	8.8461	37.203	32.544	12.870	40.667	58.312	10.686	28.093
Foreman*, i=3	2.19834	9.01273	7.05417	26.5281	25.8532	9.95975	34.476	59.0593	11.813	37.6981
Foreman*, i→∞	1.83685	6.29548	5.37842	17.9742	20.9903	8.19589	31.1571	61.8062	13.2657	53.2045
House, i=1	2348.49	557.813	565.01	478.884	296.748	337.392	191.885	96.7139	127.167	19.0444
House, i=2	2019.58	532.601	390.338	357.519	261.488	316.891	173.928	131.831	149.172	30.8287
House, i=3	1862.8	557.798	383.293	298.017	256.159	309.179	172.621	171.119	174.852	49.6032
House, i→∞	1793.37	618.417	461.923	300.508	281.494	329.983	196.109	225.406	210.326	83.8993

In Tables 2 and 3, the Degree 2 (Kale 5/3) wavelet is seen to provide more credible decorrelation results (i.e. it has better low pass/high pass variance ratios) than the Degree 1 (Daub 5/3) wavelet. On the other hand, in the third-level decomposition, Degree 3 and Degree $i \to \infty$ wavelets provide lower variances than the Daub 5/3 wavelet for LLLH, LLHL, and LLHH. On the test image *House*, the proposed wavelets provide lower variances than the Daub 5/3 wavelet for LLHL and LLHH, while on the *Ruler*, the proposed wavelets give lower

Table 3. Variances of the wavelet tree images after three level decomposition (Images 9-16).

Test Image, Degree i	LLLL	LLLH	LLHL	LLHH	LLH	LHL	LHH	LH	HL	HH
Lena, i=1	2464.13	272.89	518.885	490.206	122.431	212.094	138.107	21.9546	46.9018	21.1248
Lena, i=2	2253.33	157.469	362.422	330.592	120.968	209.867	119.307	31.2051	64.3419	29.632
Lena, i=3	2101.45	135.062	343.814	273.065	120.744	213.289	122.743	41.5706	85.733	43.404
Lena, i→∞	2008.84	161.18	408.508	276.037	131.344	239.605	147.279	55.5454	115.941	68.5239
Lena*, i=1	0.01251	0.02472	0.01225	0.05748	0.06479	0.02912	0.10691	0.07247	0.03463	0.10023
Lena*, i=2	0.01033	0.01731	0.00819	0.03913	0.04807	0.02109	0.08784	0.07151	0.03423	0.11957
Lena*, i=3	0.00848	0.01221	0.00555	0.02665	0.03748	0.01607	0.07378	0.07232	0.03428	0.14523
Lena*, i→∞	0.00723	0.00901	0.00402	0.01915	0.03018	0.01245	0.06454	0.07545	0.03486	0.18541
Mandrill, i=1	1408.32	544.516	610.79	1253.65	459.305	850.513	950.538	187.441	572.74	156.942
Mandrill, i=2	1248.15	345.986	400.348	825.676	379.435	678.221	784.919	218.704	616.323	202.834
Mandrill, i=3	1153.36	269.262	334.074	599.906	332.973	554.816	708.831	252.668	662.079	299.753
Mandrill, i→∞	1108.98	258.217	328.642	500.912	315.907	483.293	708.891	299.574	734.694	475.89
Mandrill*, i=1	0.01889	0.02714	0.03419	0.09875	0.07832	0.10237	0.23089	0.09852	0.14420	0.21238
Mandrill*, i=2	0.01572	0.01949	0.02668	0.06299	0.05796	0.07552	0.18036	0.09832	0.14050	0.25232
Mandrill*, i=3	0.01304	0.01348	0.01914	0.04212	0.04356	0.05614	0.15059	0.09836	0.13983	0.30732
Mandrill*, i→∞	0.01119	0.00971	0.01323	0.02989	0.03328	0.04195	0.13185	0.10006	0.14281	0.39427
Peppers, i=1	3090.76	413.967	403.286	254.218	141.06	162.715	82.4316	26.875	31.1291	20.0732
Peppers, i=2	2833.27	309.113	224.123	198.988	147.07	162.443	76.6928	39.4183	43.0221	23.4969
Peppers, i=3	2638.11	302.576	203.14	172.552	162.576	164.737	79.1569	54.456	56.4512	31.572
Peppers, i→∞	2508.73	366.211	257.88	193.348	195.989	182.596	93.1009	75.4749	75.1189	46.9371
Ruler, i=1	496.437	649.295	647.757	670.04	7368.59	7188.88	2342.07	2826.18	2771.34	527.882
Ruler, i=2	399.439	867.421	915.513	308.622	5431.19	5262.7	1970.89	3608.94	3557.94	651.943
Ruler, i=3	484.767	913.519	956.509	200.192	3911.56	3767.3	1442.12	4579.4	4515.96	879.277
Ruler, i→∞	508.005	961.088	980.776	175.073	2566.08	2452.02	1031.23	5935.24	5859.56	1289.55
Sailboat, i=1	4492.7	701.039	741.515	790.858	230.075	276.786	205.657	69.6518	91.1597	83.4426
Sailboat, i=2	4126.54	520.709	519.342	560.864	236.577	264.346	193.951	101.328	129.34	101.095
Sailboat, i=3	3877.02	475.044	463.289	466.511	265.965	276.485	201.277	135.318	168.296	128.493
Sailboat, i→∞	3723.56	516.835	514.574	470.951	322.877	318.592	241.197	181.208	220.763	176.458
Tank, i=1	758.424	245.605	269.936	177.249	124.279	146.336	104.447	36.6123	52.689	36.8455
Tank, i=2	685.756	105.309	124.1	127.275	111.903	129.876	86.7573	40.9287	59.5856	49.0407
Tank, i=3	626.389	73.6693	93.5861	97.9967	103.485	119.114	79.9073	47.1095	67.546	65.93
Tank, i→∞	595.779	92.8755	116.832	90.2886	103.463	118.359	83.3077	56.312	79.2899	93.9844

variance than the Daub 5/3 wavelet for only the LLHH outcome. The lower variances on the high pass end is desired. In the third-level decomposition, the variance of LLLL outcome also decreases (which is desired to increase) for Degree 1-2-3 wavelets, but lower variances achieved on the LLLH, LLHL, and LLHH compensate this drawback. If the reader carefully looks at the L/H ratios like LLLL/LLHH, it will be seen that better performance (greater ratio) is given by the proposed Degree 3 and Degree $i \to \infty$ wavelets.

In the second-level decomposition, on some images, Degree 3 and Degree $i \to \infty$ wavelets yield lower variances than the Daub 5/3 wavelet such as *Aerial* (for LLH and LHL), 2nd, *Plane* (for LLH, LHL, and LHH), *Barbara* (for LLH, LHL, and LHH), *Bus* (for LLH, LHL, and LHH).

None of the proposed wavelets provided lower variances than the Daub 5/3 wavelet for the first-level decomposition. However, as mentioned in the above paragraphs, for latter decompositions, the results are

better compared to the Daub 5/3 wavelet. Thus, the proposed wavelets Degree 3 and Degree $i \to \infty$ can be a better tool (i.e. provide better decorrelation results) for two- and three level-lifting decompositions than the Degree 1 (Daub 5/3) and Degree 2 (Kale 5/3) wavelets.

7. Conclusions

The main contribution of this research is to develop a formula for computationally efficient realizations of prediction and update filters in the lifting scheme. A general formula is provided for the users for all subband or lifting schemes.

For all cases, the prediction and update implementation on the lifting scheme consists of simple bitwise shifts and additions. However, it must be underlined that as the degree increases, the number of bitwise shifts increases as well. As for higher degrees, the wavelets in the subband decomposition scheme converge to much simpler bitwise shifts and additions as the degree goes to infinity.

The proposed wavelets are tried on 16 test images. Although they cannot outperform Daub 5/3 wavelet in the first wavelet decomposition, on some images they have performed credible compared to the Daub 5/3 wavelet in the second-level wavelet decompositions. On the other hand, the proposed wavelets performed better in the third-level wavelet decompositions. The variance at the LLLL outcome also decreases (which is meant to increase), but as mentioned previously, the low variances achieved at LLLH, LLHL, and LLHH compensate this disadvantage and provide better performance (greater LLLL/LLHH ratio).

The computationally efficient wavelets are designed exclusively for the lifting scheme. In addition to the lifting scheme wavelets, their subband decomposition scheme counterparts are also provided; however, subband decomposition realizations cannot be implemented using simple bitwise shifts. The convenience of the lifting scheme is understood once again in this research.

References

[1] Sweldens W. The lifting scheme: a custom-design construction of biorthogonal wavelets. Applied and Computational Harmonic Analysis 1996; 3(2): 186-200. doi: 10.1006/acha.1996.0015

[2] Sweldens W. The lifting scheme: A construction of second generation wavelets. SIAM Journal of Mathematical Analysis 1997; 29(2): 511-546. doi: 10.1137/S0036141095289051

[3] Daubechies I, Sweldens W. Factoring wavelet transforms into lifting steps. Journal of Fourier Analysis and Applications 1998; 4(3): 247-269. doi: 10.1007/BF02476026

[4] Gerek ÖN, Cetin AE. A 2-D orientation-adaptive prediction filter in lifting structures for image coding. IEEE Transactions on Image Processing 2006; 15(1): 106-111. doi: 10.1109/TIP.2005.859369

[5] Gerek ÖN, Cetin AE. Adaptive polyphase subband decomposition structures for image compression. IEEE Transactions on Image Processing 2000; 9(10): 1649-1660. doi: 10.1109/83.869176

[6] Cetin AE, Gerek ÖN, Ulukus S. Block wavelet transforms for image coding. IEEE Transactions on Circuits and Systems for Video Technology 1993; 3(6): 433-435. doi: 10.1109/76.260200

[7] Kale MC, Atac G, Gerek ÖN. A biorthogonal wavelet design technique using Karhunen-Loéve Transform approximation. Digital Signal Processing 2016; 51(4): 202-222. doi: 10.1016/j.dsp.2015.06.002

[8] Kale MC, Gerek ÖN. Lifting wavelet design by block wavelet transform inversion. In: IEEE ICASSP; Florence, Italy; 2014. pp. 2619-2623. doi: 10.1109/ICASSP.2014.6854074

[9] Kale MC. A general biorthogonal wavelet based on Karhunen-Loéve transform approximation. Signal, Image and Video Processing 2016; 10(4): 791-794. doi: 10.1007/s11760-016-0860-2

[10] Adams MD, Kossentni F. Reversible integer-to-integer wavelet transforms for image compression: performance evaluation and analysis. IEEE Transactions on Image Processing 2000; 9(6): 101-1024. doi: 10.1109/83.846244

[11] Calderbank AR, Daubechies I, Sweldens W, Yeo BL. Wavelet transforms that map integers to integers. Applied and Computational Harmonic Analysis 1998; 5(3): 332-369. doi: 10.1006/acha.1997.0238

[12] Calderbank AR, Daubechies I, Sweldens W, Yeo BL. Lossless image compression using integer to integer wavelet transforms. In: Proceedings of IEEE International Conference Image Processing, vol. 1; Santa Barbara, CA, USA; 1997. pp. 596-599.

[13] Said A, Pearlman WA. An image multiresolution representation for lossless and lossy compression. IEEE Transactions on Image Processing 1996; 5(9): 1303-1310. doi: 10.1109/83.535842

[14] Memon N, Wu X, Yeo BL. Improved techniques for lossless image compression with reversible integer wavelet transforms. In: Proc. IEEE International Conference Image Processing, vol. 3; Chicago, IL; 1998. pp. 891 -895

[15] Sersic D. Integer to integer mapping wavelet filter bank with adaptive number of zero moments. In: IEEE ICASSP; Istanbul, Turkey; 2000. pp.1-25.

[16] Toreyin BU, Yilmaz O, Mert YM. Evaluation of on-board integer wavelet transform based spectral decorrelation schemes for lossless compression of hyperspectral images. In: 6th Workshop on Hyperspectral Image and Signal Processing: Evolution in Remote Sensing (WHISPERS); Lausanne, Switzerland; 2014. pp.1-20.

[17] Liu Z, Zheng N. Parametrization construction of biorthogonal wavelet filter banks for image coding. Signal Image and Video Processing 2007; 1(1): 63-76. doi: 10.1007/s11760-007-0001-z

[18] Liu Z, Gao C. Construction of parametric biorthogonal wavelet filter banks with two parameters for image coding. Signal Image and Video Processing 2008; 2(3): 195-206. doi: 10.1007/s11760-008-0050-y

[19] Zhu HI, Shen JJ, Dai Z, Song W, Chang ZX. Single-channel source separation and parameters estimation of multi-component BPSK/QPSK signal based on 3-D EVR spectrum and wavelet analysis. Signal Image and Video Processing 2019; 1:1-20. doi: 10.1007/s11760-019-01500-w

[20] Cohen A, Daubechies I, Feauveau JC. Biorthogonal bases of compactly supported wavelets. Communications on Pure and Applied Mathematics 1992, 45(5): 485-560, doi: 10.1002/cpa.3160450502

[21] Patil PB, Chavan MS. A wavelet based method for denoising of biomedical signal. In: International Conference on Pattern Recognition, Informatics and Medical Engineering (PRIME-2012); Salem, Tamilnadu, India; 2012. pp. 278-283.

[22] Patil B, Patwardhan P, Gadre V. A generalized approach for finite precision 5/3 filter designs. In: Proceedings of National conference on Communications NCC; New York, USA; 2007. pp. 112-115.

[23] Le Gall D, Tabatabai A. Sub-band coding of digital images using symmetric short kernel filters and arithmetic coding technique. In: IEEE ICASSP; New York, USA; 1988. pp. 761-764, doi: 10.1109/ICASSP.1988.196696